

A theory of double exchange in infinite dimensions

B.M. Letfulov^a

Institute of Metal Physics, Ural division of Russian Academy of Sciences, Kovalevskaya str. 18, Ekaterinburg 620219, Russia

Received: 24 January 1997 / Revised: 14 February 1997 / Received in final form: 18 August 1997 / Accepted: 25 August 1997

Abstract. This paper gives a simplified model of the double exchange which is a kind of indirect exchange interaction between localized magnetic moments. The presented model is solved exactly in the case of infinite – dimensional space. Equations for single-particle Green’s function and magnetization of the localized spins subsystem are obtained. It is shown that our simple double exchange model reveals an instability to the ferromagnetic ordering of localized moments. Magnetic and electric properties of this system on Bethe lattice with $z = \infty$ are investigated in detail.

PACS. 71.27.+a Strongly correlated electron systems; heavy fermions – 68.35.Rh Phase transitions and critical phenomena – 72.10.-d Theory of electronic transport; scattering mechanisms

1 Introduction

The double exchange is one of the forms of indirect exchange interaction between localized magnetic moments *via* itinerant electrons [1–6]. Historically it arose in connection with experimental study of magnetic perovskites $\text{La}_{1-x}\text{M}_x\text{MnO}_3$, where $\text{M} = \text{Ca}, \text{Sr}, \text{Ba}, \text{Cd}$ [7], and with the ascertainment of the close connection between electric and magnetic properties of these substances. In [7] it was demonstrated that with the replacement of three-valent ions La^{3+} by two-valent ions M^{2+} there appears ferromagnetic ordering in the system, and at $x \geq 0.3$ the dielectric phase changes by the metallic one, and under it the saturated magnetization and Curie temperature grow rapidly with the increasing concentration of admixture ions M. Zener [8] explained this connection between the appearance of ferromagnetism and conductivity with the help of the so called double exchange, which is organically connected with the transfer of charge from one magnetic ion to another. The point is that in mixed manganites the substitution of three-valent ion La^{3+} by two-valent ion Mn^{3+} to the Mn^{4+} state. The newly appeared additional electron (Zener electron) is in an itinerant state and three d -electrons of ion Mn^{4+} form a localized magnetic moment. In this case, because of strong exchange interaction between Zener electron and localized moment, the Zener electron spin is always parallel (antiparallel) to the localized spin. This circumstance is very essential for the establishment of long-range magnetic ordering in the system because of the fact that the Zener electron transfers from one magnetic ion to another without change of its spin projection. Thus, the transfer of additional electrons from

one manganese ion to another results in both appearance of metallic conductivity in mixed manganites and establishment of ferromagnetic ordering.

Usually the double exchange mechanism is considered in the scope of an $s-f$ exchange model which was first defined by Vonsovsky in 1946 [9]. Sometimes it is named the Kondo lattice. This model assumes the existence of localized magnetic moments in the system (f -subsystem) and itinerant electrons (s -subsystem) which are connected among themselves by an intra-atomic exchange interaction. The Hamiltonian of this model looks like:

$$\mathcal{H} = \mathcal{H}_0 + \mathcal{H}_{int}, \quad (1.1)$$

$$\mathcal{H}_0 = \sum_{g,\sigma} \varepsilon_\sigma a_{g\sigma}^\dagger a_{g\sigma} - \frac{1}{2} H \sum_g S_g^z + \sum_{g,g',\sigma} t_{gg'} a_{g\sigma}^\dagger a_{g'\sigma}, \quad (1.2)$$

$$\mathcal{H}_{int} = -\frac{1}{2} I \sum_g \left\{ \alpha (S_g^+ a_{g\downarrow}^\dagger a_{g\uparrow} + S_g^- a_{g\uparrow}^\dagger a_{g\downarrow}) + \beta S_g^z (a_{g\uparrow}^\dagger a_{g\uparrow} - a_{g\downarrow}^\dagger a_{g\downarrow}) \right\}, \quad (1.3)$$

where $\varepsilon_\sigma = -\mu - \sigma H/2$, H is the external magnetic field, S_g is the operator of localized spin at the site with number g , α and β are the coefficients of anisotropy of $s-f$ exchange interaction.

Double exchange is realized in those materials whose $s-f$ exchange parameter I is much more than the average kinetic energy of itinerant electrons. This circumstance introduces significant difficulties for constructing the double exchange theory. The correct Hamiltonian of the double exchange, defined by Kubo and Ohata in [3] and obtained from (1.1) at $\alpha = \beta = 1$ in the limit $I \rightarrow \infty$, is so complicated that we can use only very rough approximation

^a e-mail: Barri.Letfulov@imp.uran.ru

methods for the investigation of double exchange in terms of this Hamiltonian.

In connection with this appears a question about construction and investigation of a simplified double exchange model which would contain the basic peculiarities of the phenomenon under consideration.

Recently, Furukawa [10–14] has studied some magnetic and transport properties of perovskite-type manganese oxides $\text{La}_{1-x}\text{M}_x\text{MnO}_3$ on the basis of the isotropic s - f model with the localized spins treated in the classical approximation ($S \rightarrow \infty$). Using this simplification Furukawa has obtained the exact expression for the single-particle Green's function in infinite dimensions, and in the limit of large I was able to explain the temperature behaviour of magnetoresistance in the mentioned materials.

In the present paper we have considered the s - f model with the quantum localized spins ($S = 1/2$) and in Section 2 we shall introduce the simplified model of double exchange which was studied at first in [6]. In Section 3 this model will be solved exactly in the infinite-dimensional space by the diagrammatic technique. Equations obtained in this section defining single-particle Green's function will be solved in Section 4 for Bethe lattice with $z \rightarrow \infty$ (z is the nearest neighbours number). In this section we shall obtain too the equation for the magnetization of the f -subsystem, and magnetic properties of Bethe lattice with $z \rightarrow \infty$ will be investigated. Transport properties (a resistivity) of Bethe lattice will be studied in Section 5. The general discussion of the obtained results will be given in the last section.

2 The simplified model of double exchange

Consider the s - f model Hamiltonian (1.1) with $S = 1/2$. The basic physical peculiarity of double exchange which causes the ferromagnetic ordering of localized spins is the parallelism (or antiparallelism) of itinerant electron spin and localized spin at each site. We can conserve this peculiarity in the double exchange Hamiltonian, if, deriving it, we start from (1.3) where we put $\alpha = 0$, $\beta = 1$. Thus, we take that

$$\mathcal{H}_{int} = -\frac{1}{2}I \sum_g S_g^z (a_{g\uparrow}^\dagger a_{g\uparrow} - a_{g\downarrow}^\dagger a_{g\downarrow}) \quad (2.1)$$

where let it be that $S_g^z S_g^z = 1$.

Let us introduce Fermi type operators

$$c_{1g\sigma} = \frac{1}{2}(1 + \sigma S_g^z) a_{g\sigma}, \quad c_{2g\sigma} = \frac{1}{2}(1 - \sigma S_g^z) a_{g\sigma}, \quad (2.2)$$

$$\{c_{ng\sigma}, c_{n'g'\sigma'}^\dagger\} = \frac{1}{2}(1 \pm \sigma S_g^z) \delta_{nn'} \delta_{gg'} \delta_{\sigma\sigma'} \quad (2.3)$$

such that

$$[\mathcal{H}_{int}, c_{1g\sigma}] = -\frac{1}{2}I, \quad [\mathcal{H}_{int}, c_{2g\sigma}] = \frac{1}{2}I. \quad (2.4)$$

It is seen from equations (2.2–2.4) that the c -operators describe complexes consisting of the localized spin and the itinerant electron. And the itinerant electron spin is parallel (antiparallel) to the localized spin in the complex, described by the operator $c_{1g\sigma}$ ($c_{2g\sigma}$). The energies $-I/2$ and $I/2$ determine one-site levels of the corresponding complexes.

As

$$c_{1g\sigma} + c_{2g\sigma} = a_{g\sigma}, \quad (2.5)$$

the operator in (1.2) responsible for the transfer of itinerant electrons from site to site, in terms of c -operators will look like

$$\sum_{n,n'} \sum_{g,g',\sigma} t_{gg'} c_{ng\sigma}^\dagger c_{n'g'\sigma}. \quad (2.6)$$

Thus, in the limit $I \rightarrow \infty$ only the part of (2.6) which is responsible for the transfer of itinerant electrons with the spin parallel to localized spin, have the sense. As the result for the double exchange Hamiltonian we have

$$\mathcal{H}_{d.ex} = \mathcal{H}_0 + \mathcal{H}_{int}, \quad (2.7)$$

$$\mathcal{H}_0 = -\frac{1}{2}H \sum_g S_g^z - \mu \sum_{g\sigma} c_{1g\sigma}^\dagger c_{1g\sigma}, \quad (2.8)$$

$$\mathcal{H}_{int} = \sum_{g,g',\sigma} t_{gg'} c_{1g\sigma}^\dagger c_{1g'\sigma}. \quad (2.9)$$

We shall omit the index “1” for c -operators in the future. For calculation of magnetization of the f -subsystem we suggest that the magnetic field H act on the f -subsystem only. The summation in (2.9) is taken over the nearest neighbours. Therefore

$$t_{gg'} = t \sum_\rho \delta_{g+\rho,g'}, \quad \mathbf{R}_{g+\rho} = \mathbf{R}_g + \Delta_\rho, \quad (2.10)$$

where Δ_ρ is the radius-vector of the nearest neighbour with number ρ .

In the infinite-dimensional space the process of scaling of constant t sets with the help of relation [15, 16]

$$t \rightarrow \frac{t^*}{2\sqrt{d}}, \quad t^* = \text{const} \quad (2.11)$$

where d is a space dimension. In Bethe lattice with infinite number of the nearest neighbours case ($z = \infty$) the scaling sets also with the help of (2.11), where it should be put $d = z/2$, so that $t \rightarrow t^*/\sqrt{2z}$.

Comparing (2.7) with the Hamiltonian of Kubo and Ohata one can easily see that we entirely neglected processes with the turnover of the spin. Moreover an itinerant electron, described by our Hamiltonian, when transferred from one magnetic site to another does not feel there is on the latter an electron with opposite spin projection or not. The first restriction is essential for the low temperature region where it is important to consider the spin-wave excitations. So we shall pretend only to describe qualitatively the magnetic properties of ferromagnets with the

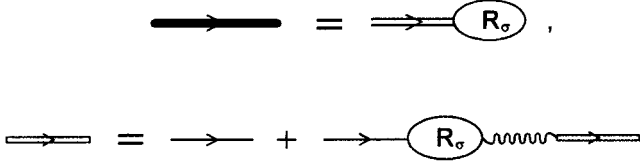


Fig. 1. General diagram structure of the single-particle Green's function $\mathcal{G}_\sigma(g, g'; \tau - \tau')$.

double exchange. What about the second restriction, it is not essential for materials with small concentration of itinerant electrons or holes. Magnetic semiconductors are such materials, for example doped europium halcogenides [17].

It should be pointed out in connection with this that the simplicity of Hamiltonian (2.7) may be found essential for obtaining exact results which are of major interest in the theory of many particle systems. In particular, a model with Hamiltonian (2.7) is resolved exactly in the infinite-dimensional space, and obtained results prove to be relatively simple.

3 Double exchange in the infinite-dimensional space

In this section, exact equations will be given for a single-particle Green's function and magnetization of a localized spins subsystem for a model with Hamiltonian (2.7) in infinite dimensions. In this connection we shall use the diagram technique for c -operators that was developed in [6]. In virtue of anticommutation relations (2.3) this technique is similar to diagram techniques for Hubbard X -operators (see, for instance [18]), but it is considerably simpler in a set of internal vertices.

The general diagram structure of the single-particle Green's function

$$\mathcal{G}_\sigma(g, g'; \tau - \tau') = -\langle T_\tau \tilde{c}_{g\sigma}(\tau) \tilde{c}_{g'\sigma}^\dagger(\tau') \rangle \quad (3.1)$$

is shown in Figure 1, where transfer integral $t_{gg'}$ associates with the wavy line and “zero” Green's function

$$G_\sigma^0(g, g'; i\omega_k) = \frac{\delta_{gg'}}{i\omega_k + \mu} = G_\sigma^0(i\omega_k) \delta_{gg'} \quad (3.2)$$

is associated with the thin solid line.

It is seen from Figure 1 that in contrast to the usual diagram technique for standard Fermi operators the expression for function (3.1) contains so-called “end” part $R_\sigma(g, g'; \tau - \tau')$, so that

$$\mathcal{G}_\sigma(g, g'; i\omega_k) = \sum_{g_1} G_\sigma(g, g_1; i\omega_k) R_\sigma(g_1, g'; i\omega_k), \quad (3.3)$$

where $G_\sigma(g, g'; i\omega_k)$, represented in Figure 1 by double solid line, obeys the usual Dyson equation

$$G_\sigma(g, g'; i\omega_k) = G_\sigma^0(g, g'; i\omega_k) + \sum_{g_1, g_2} G_\sigma^0(g, g_1; i\omega_k) \Xi_\sigma(g_1, g_2; i\omega_k) G_\sigma(g_2, g'; i\omega_k), \quad (3.4)$$

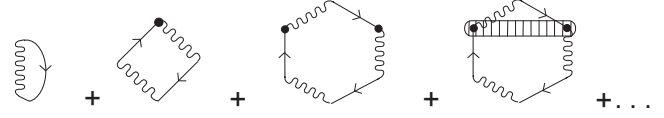


Fig. 2. Diagram series for $P_\sigma(i\omega_k)$.

where

$$\Xi_\sigma(g, g'; i\omega_k) = \sum_{g_1} R_\sigma(g, g_1; i\omega_k) t_{g_1 g'}. \quad (3.5)$$

We shall consider that

$$R_\sigma(g, g'; i\omega_k) = R_\sigma(g, g; i\omega_k) \delta_{gg'} \equiv R_\sigma(i\omega_k) \delta_{gg'}, \quad (3.6)$$

according to the general ideology of the theory of itinerant electron systems in infinite-dimensional space [15, 16]. Then the expression for the local single-particle Green's function gains the view

$$\mathcal{G}_\sigma(g, g'; i\omega_k) \equiv \mathcal{G}_\sigma(i\omega_k) = R_\sigma(i\omega_k) G_\sigma(i\omega_k), \quad (3.7)$$

where

$$G_\sigma(i\omega_k) \equiv G_\sigma(g, g; i\omega_k) = \int_{-\infty}^{\infty} \frac{dx \rho_0(x)}{i\omega_k + \mu - R_\sigma(i\omega_k) x} \quad (3.8)$$

and

$$\rho_0(\varepsilon) = \frac{1}{N} \sum_{\mathbf{k}} \delta(\varepsilon - \varepsilon(\mathbf{k})) \quad (3.9)$$

is the density of single-particle states.

Let's find the equation for “end” part $R_\sigma(i\omega_k)$. It's suitable for this purpose to use diagram expansion of the other function

$$P_\sigma(g, g; i\omega_k) \equiv P_\sigma(i\omega_k) = \int_{-\infty}^{\infty} \frac{dx x \rho_0(x)}{i\omega_k + \mu - R_\sigma(i\omega_k) x} \quad (3.10)$$

which is connected with (3.8) by the relation

$$G_\sigma(i\omega_k) = G_\sigma^0(i\omega_k) [1 + P_\sigma(i\omega_k) R_\sigma(i\omega_k)] \quad (3.11)$$

because of peculiarities of the structure of diagram series for $\mathcal{G}_\sigma(i\omega_k)$. It is seen from (3.11) that the function $P_\sigma(i\omega_k)$ is of the zero'th order with the respect to parameter $1/d$.

Diagrams, taking into account $P_\sigma(i\omega_k)$, are shown in Figure 2 where unshaded ovals with the n bold points inside correspond to zero-order cumulants:

$$\begin{aligned} \begin{array}{c} \bullet \quad \bullet \quad \bullet \\ \hline i_1 \quad i_2 \quad i_n \end{array} &\equiv D_\sigma^0(i_1, i_2, \dots, i_n) \\ &= \left(\frac{1}{2}\sigma\right)^n \frac{\partial^{n-1}}{\partial y_0^{n-1}} b(y_0) \delta_{i_1 i_2} \delta_{i_2 i_3} \dots \delta_{i_{n-1} i_n}, \end{aligned} \quad (3.12)$$

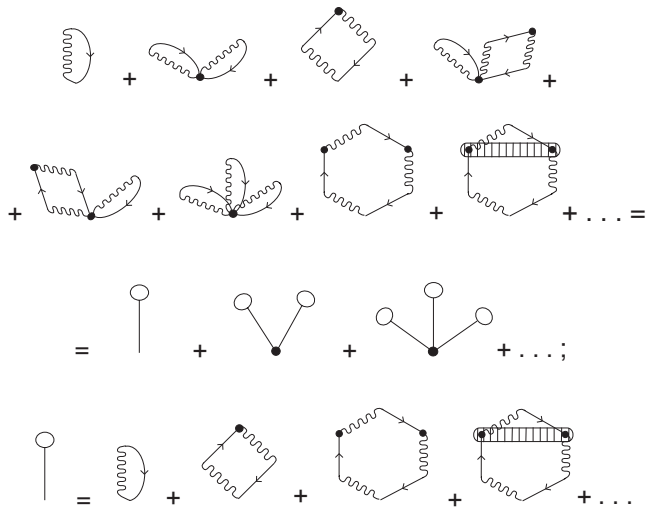


Fig. 3. Rebuilt series for $P_\sigma(i\omega_k)$ and a diagram series for $\mathcal{P}_\sigma(i\omega_k)$.

$$b(y_0) = \langle S_g^z \rangle_0 = \tanh(y_0), \quad y_0 = \frac{1}{2} \frac{H}{T}. \quad (3.13)$$

The series in Figure 2 is a sum of diagrams with external vertices having equal site indices and with all possible cumulant bonds replaced with those ones taken in the exact local approximation. These exact local cumulants $D_\sigma(g_1, g_2, \dots, g_n)$ are presented in Figure 2 by shaded ovals with n bold points inside.

The possibility of the exact calculation of the cumulants in local approximation is caused by the fact that

$$[\mathcal{H}_{d.ex}, S_g^z] = 0$$

and that the exact average of the T_τ -product of operators $(1 + \sigma S_g^z)$ taken in Heisenberg presentation does not depend on Matsubara times. An analogous situation takes place in the exactly solved infinite-dimensional space Falicov-Kimball model [19].

Thus,

$$\bullet \equiv D_\sigma(g) = \frac{1}{2}(1 + \sigma m),$$

$$\bullet \bullet \equiv D_\sigma(g_1, g_2) = \frac{1}{4}(1 - m^2)\delta_{g_1 g_2} \quad (3.14)$$

$$\bullet \bullet \bullet \equiv D_\sigma(g_1, g_2, g_3) = -\frac{1}{4}\sigma m(1 - m^2)\delta_{g_1 g_2}\delta_{g_2 g_3}$$

and so on, where m is the magnetization of the local spins subsystem. All these formulae are easily calculated with the help of (3.12) and (3.13) with the change of $b(y_0)$ by m . The exact equation for m will be given later.

To sum the series in Figure 2 let us rebuild it, so that as a result we can obtain the series shown in Figure 3. For this, taking into account the circumstance that the summation is taken over coordinates (lattice sites) of internal vertices, we select in each diagram in Figure 2 the contributions with internal vertices coinciding by coordinate with external vertex in every possible way. It is necessary

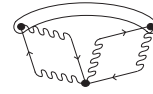


Fig. 4. Diagrams of this type equal to zero at limit $d \rightarrow \infty$.

to use relations (3.14) when combining. Thus, in Figure 3 at the first, third, seventh and eighth diagrams of the series for $P_\sigma(i\omega_k)$ none of the internal vertices can coincide with external vertex, and the magnitude $\mathcal{P}_\sigma(i\omega_k)$, shown in the same figure, is the sum of the diagrams of just such a type.

After the mentioned rebuilding, graphs of the type shown in Figure 4 turn out to be omitted in Figure 3. But they are equal to zero in the limit $d \rightarrow \infty$ or $z \rightarrow \infty$, because diagrams of such a type have at least one pair of internal vertices that are connected by local cumulants.

The series for $P_\sigma(i\omega_k)$ in Figure 3 is summed easily in terms of functions $\mathcal{P}_\sigma(i\omega_k)$:

$$P_\sigma(i\omega_k) = \mathcal{P}_\sigma(i\omega_k) \frac{1 - \frac{1}{2}(1 - \sigma m)\mathcal{P}_\sigma(i\omega_k)}{1 - \mathcal{P}_\sigma(i\omega_k)}. \quad (3.15)$$

It is easy to see that function $P_\sigma(g, g'; i\omega_k)$ obeys the equation

$$P_\sigma(g, g'; i\omega_k) = P_\sigma^0(g, g'; i\omega_k) + R_\sigma(i\omega_k) \sum_{g_1} P_\sigma^0(g, g_1; i\omega_k) P_\sigma(g_1, g'; i\omega_k) \quad (3.16)$$

where

$$P_\sigma^0(g, g'; i\omega_k) = \frac{t_{gg'}}{i\omega_k + \mu}. \quad (3.17)$$

The last equation can be obtained from Dyson equation (3.4) by way of multiplying it by $t_{g''g}$ and summing over g .

Equation (3.16) gives us an opportunity to get an equation for $\mathcal{P}_\sigma(i\omega_k)$. Indeed, taking into account the method of construction of this function, it is not difficult to show that function $\mathcal{P}_\sigma(i\omega_k)$ must obey equation

$$\mathcal{P}_\sigma(g, g'; i\omega_k) = P_\sigma^0(g, g'; i\omega_k) + R_\sigma(i\omega_k) \sum_{g_1 \neq g'} P_\sigma^0(g, g_1; i\omega_k) \mathcal{P}_\sigma(g_1, g'; i\omega_k), \quad (3.18)$$

where in contrast with (3.16) the second term of the right part has a restriction in summation over g_1 .

After Fourier transformation we can obtain from (3.18)

$$\mathcal{P}_\sigma(i\omega_k) = \frac{P_\sigma(i\omega_k)}{1 + R_\sigma(i\omega_k)P_\sigma(i\omega_k)}. \quad (3.19)$$

By substituting (3.19) into (3.15) we obtain the desired equation for $R_\sigma(i\omega_k)$:

$$R_\sigma(i\omega_k) = \frac{\frac{1}{2}(1 + \sigma m)}{1 + P_\sigma(i\omega_k)[R_\sigma(i\omega_k) - 1]}. \quad (3.20)$$

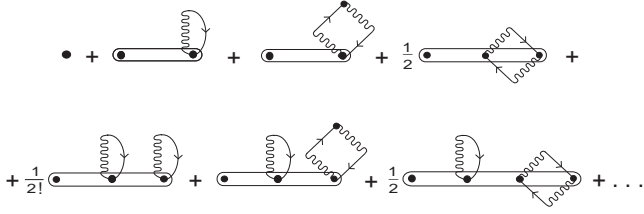


Fig. 5. Diagram series for the magnetization m .

If taking into account that $P_\sigma(i\omega_k)$ is connected with function $G_\sigma(i\omega_k)$ by relation (3.11), so equations (3.8, 3.20) are the system of equations for finding $R_\sigma(i\omega_k)$, $G_\sigma(i\omega_k)$ and consequently $\mathcal{G}_\sigma(i\omega_k)$.

For the calculation of magnetization of the localized spins subsystem

$$m = \langle S_g^z \rangle = \frac{\langle \tilde{S}_g^z(\tau) \sigma(\beta) \rangle_0}{\langle \sigma(\beta) \rangle_0} \quad (3.21)$$

let us examine the series, shown in Figure 5. After rebuilding this series, analogous in practice to the one done for function $P_\sigma(g, g; i\omega_k)$ it is possible to obtain the series shown in Figure 6. This series is a Taylor series and is summed up easily. As a result we obtain

$$m = \tanh(y_0 + \eta), \quad (3.22)$$

$$\eta = \sum_{\omega_k} \ln \frac{1 - \mathcal{P}_\uparrow(i\omega_k)}{1 - \mathcal{P}_\downarrow(i\omega_k)}. \quad (3.23)$$

The magnitude η is an internal field (molecular field) with which itinerant electrons are acting on localized spins subsystem. Since $\eta \neq 0$ only when $m \neq 0$, (3.22) is a self-consistent equation for m .

4 Bethe lattice. Magnetic properties

For Bethe lattice with $z \rightarrow \infty$ the system of equations (3.8) and (3.20) can be solved and we can get an explicit expression for $\mathcal{G}_\sigma(i\omega_k)$. Indeed, taking into account that the density of single-particle states $\rho_0(\varepsilon)$ has in this case the form

$$\rho_0(\varepsilon) = \frac{4}{\pi W} \sqrt{1 - \left(\frac{2\varepsilon}{W}\right)^2}, \quad -\frac{1}{2}W < \varepsilon < \frac{1}{2}W, \quad (4.1)$$

where $W = 2\sqrt{2}t^*$, we easily take an integral in (3.8) and for $G_\sigma(i\omega_k)$ we obtain

$$G_\sigma(i\omega) = 2 \left\{ i\omega_k + \mu + \sqrt{(i\omega_k + \mu)^2 - \frac{1}{4}W^2 R_\sigma^2(i\omega_k)} \right\}^{-1}. \quad (4.2)$$

Substituting in (4.2) the expression for $R_\sigma(i\omega_k)$

$$R_\sigma(i\omega_k) = \frac{G_\sigma(i\omega_k) - \frac{1}{2}(1 - \sigma m)G_\sigma^0(i\omega_k)}{G_\sigma(i\omega_k)} \quad (4.3)$$

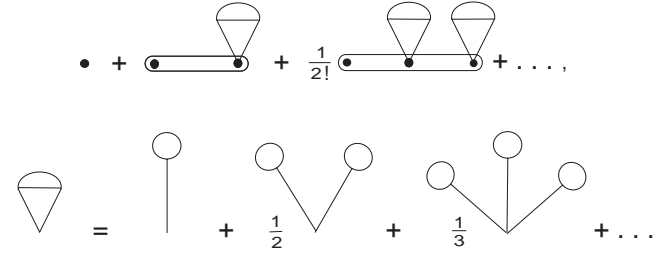


Fig. 6. Rebuilt series for the magnetization m .

obtained with the help of equations (3.11, 3.20), we easily get the equation for $G_\sigma(i\omega_k) \equiv G_\sigma$:

$$G_\sigma^2 - 2 \left[\frac{8}{W^2}(i\omega_k + \mu) + \frac{1}{2}(1 - \sigma m)G_\sigma^0 \right] G_\sigma + \frac{16}{W^2} + \frac{1}{4}(1 - \sigma m)^2 (G_\sigma^0)^2 = 0. \quad (4.4)$$

We have from it

$$G_\sigma(i\omega_k) = \frac{1}{2}(1 - \sigma m)G_\sigma^0(i\omega_k) + \frac{8}{W^2} \left\{ i\omega_k + \mu - \sqrt{(i\omega_k + \mu)^2 - \frac{1}{8}W^2(1 + \sigma m)} \right\}. \quad (4.5)$$

Now it is not hard already with the help of (4.3) to obtain expressions for $\mathcal{G}_\sigma(i\omega_k)$

$$\mathcal{G}_\sigma(i\omega_k) = \frac{8}{W^2} \left\{ i\omega_k + \mu - \sqrt{(i\omega_k + \mu)^2 - \frac{1}{8}W^2(1 + \sigma m)} \right\} \quad (4.6)$$

and for $\mathcal{P}_\sigma(i\omega_k)$:

$$1 - \mathcal{P}_\sigma(i\omega_k) = \frac{1}{16}W^2 G_\sigma^0(i\omega_k) \mathcal{G}_\sigma(i\omega_k). \quad (4.7)$$

So for Bethe lattice we have

$$n = \sum_{\sigma} (1 + \sigma m) \frac{1}{\pi} \int_0^{\pi} dt \sin^2 t f(a_{\sigma} \cos t) \quad (4.8)$$

and

$$\eta = \frac{1}{\pi} \int_0^{\pi} dt \ln \left(\frac{1 + \exp[(\mu - a_{\uparrow} \cos t)/T]}{1 + \exp[(\mu - a_{\downarrow} \cos t)/T]} \right), \quad (4.9)$$

where n is the itinerant electrons' concentration,

$$a_{\sigma} = \frac{1}{2}W \sqrt{\frac{1}{2}(1 + \sigma m)} \quad (4.10)$$

is a halfwidth of the correlation conducting band and $f(z)$ is Fermi-Dirac function, $f(z) = 1/[\exp \beta(z - \mu) + 1]$. Equation (4.9) is an equation for chemical potential μ .

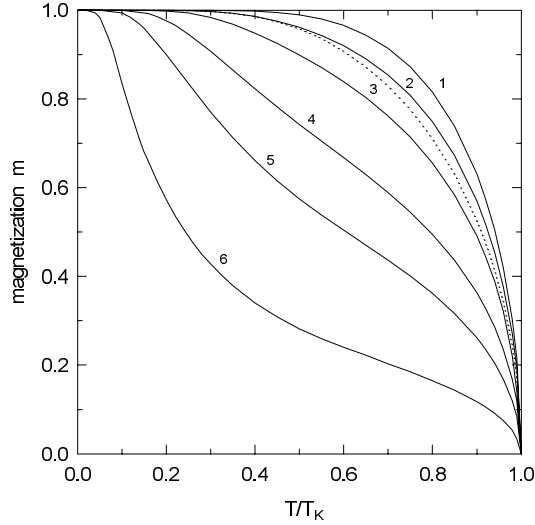


Fig. 7. Temperature dependence of the magnetization m for different electron concentration n . 1 – $n = 0.5$, 2 – $n = 0.7$, 3 – $n = 0.8$, 4 – $n = 0.9$, 5 – $n = 0.95$, 6 – $n = 0.99$. The dotted line is the mean-field curve for Heisenberg ferromagnet.

In Figure 7 the temperature dependence of magnetization for different n is shown. Comparing it with the mean-field curve for magnetization of a Heisenberg ferromagnet

$$m = \tanh\left(\frac{T_K}{T} m\right). \quad (4.11)$$

We see that at small values of $1 - n$ the magnetization values are less than they should be at given T/T_K from (4.11), and at $n = 0.5$ the magnetization curve is placed above the mean-field curve on the plot.

It should be noticed in connection with this that the temperature behaviour of the magnetization at small values of $1 - n$ with two flex points essentially differs from the behaviour of the Heisenberg mean-field curve. Analogous behaviour can be found in a Heisenberg ferromagnet with a small concentration of paramagnetic impurities. Therefore we can conclude that in a magnetic sense the double exchange system at small values of $1 - n$ presents itself as the Heisenberg ferromagnet with non-regular localized spins.

Indeed, in the $I = \infty$ case the s -electron spin so hardly is bound with the localized spin on the same site that the complex consisting of the localized spin and the itinerant electron spin is the non-regular spin. Actually, introduced in Section 2, the c -operators (c^\dagger -operators) are the operators of annihilation (creation) of the non-regular spins.

It should be noted, that the mentioned analogy between double exchange system at small values of $1 - n$ and Heisenberg ferromagnet with paramagnetic impurities was first discovered in old papers of Nagaev (see, for example, [20]).

The deviation of magnetic behavior from Heisenberg ferromagnets also appears in the temperature dependence of magnetic susceptibility which can be obtained from

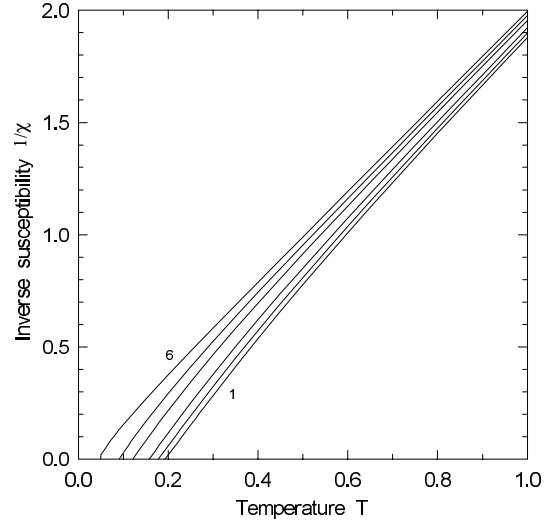


Fig. 8. Temperature dependence of inverse susceptibility for different electron concentration n . 1 – $n = 0.5$, 2 – $n = 0.7$, 3 – $n = 0.8$, 4 – $n = 0.9$, 5 – $n = 0.95$, 6 – $n = 0.99$.

(3.22) as a derivative of m with respect to H :

$$\chi = \frac{\frac{1}{2}}{T - \frac{1}{8}W^2\Pi}, \quad (4.12)$$

where

$$\Pi = -\frac{1}{\pi a} \int_{-a}^a dz \sqrt{1 - (z/a)^2} \frac{df(z)}{dz}, \quad (4.13)$$

and $a = W/2\sqrt{2}$. Indeed, the analysis of the temperature behaviour of the inverse susceptibility at various n exhibits that at $T/a \gg 1$ the susceptibility obeys Curie law for all n . At $T/a < 1$ the curvature (see Fig. 8, where $1/\chi$ and T are expressed in units of $W/2$) of the temperature dependence of χ^{-1} is opposite in sign to the one observed in Heisenberg ferromagnets. As a result the inverse susceptibility crosses temperature axes at finite temperature. It seems that here the susceptibility critical exponent $\gamma < 1$, while in the Heisenberg ferromagnet $\gamma \geq 1$ in any approximation.

The marked anomaly in the temperature behaviour of the susceptibility was pointed out long ago in Anderson and Hasegawa's work [1] where double exchange was considered in the scope of a two atom system. High-temperature expansion of susceptibility in [1] does not include the term proportional to $1/T$, which is what served the authors of the work [1] as the reason for concluding that susceptibility obeys Curie law at high temperatures, and that it has inverse curvature compared with the Heisenberg one at low temperatures. Our exact calculation with Hamiltonian (2.7) in the infinite-dimensional space confirms this qualitative conclusion.

It is possible to find from (4.12) the dependence of Curie temperature T_K on electron concentration n . This dependence is shown in Figure 9, where T_K is expressed

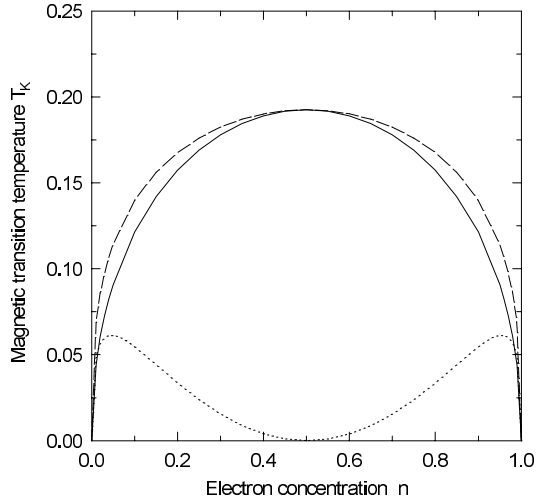


Fig. 9. Electron concentration dependence of the magnetic transition temperature T_K . The full line: T_K from the singularities of the susceptibility (4.12), the dashed line: T_K from the approximate formula (4.14), the dotted line: T_K in the Hubbard-type approximation.

in units of $W/2$. Approximately, the formula for T_K looks like the following

$$T_K = \alpha \frac{a}{\pi} \sqrt{1 - (\varepsilon_F/a)^2}, \quad (4.14)$$

where Fermi energy ε_F is defined from (4.8) at $T = 0$, and $\alpha = 0.856$ is the fitted coefficient.

Let us note that the usage of the Hubbard-I type approximation (for Hamiltonian (2.7)) gives us the next expression for T_K [6]

$$T_K = 0.5\varepsilon_F^2 \rho_0(\varepsilon_F), \quad (4.15)$$

which essentially differs from (4.14) (see Fig. 9), because at $n = 0.5$ T_K from (4.14) has a maximum and T_K from (4.15) is zero. Thus, the results of [6] remain true only when $1 - n \ll 1$ and $n \ll 1$.

Concluding this part we give formulae for the energy of the ferromagnetic state at $T = 0$ ($m = 1$)

$$E_F = -\frac{1}{3}W \frac{1}{\pi} \left[1 - \left(\frac{2\varepsilon_F}{W} \right)^2 \right]^{3/2} \quad (4.16)$$

and the paramagnetic state ($m = 0$)

$$E_P = -\frac{1}{3}W \frac{1}{\pi\sqrt{2}} \left[1 - \left(\frac{\varepsilon_F}{a} \right)^2 \right]^{3/2}. \quad (4.17)$$

It follows from equation (4.16, 4.17) that the ferromagnetic state is energetically more advantageous than the paramagnetic one at electron concentrations belonging to the interval $0 < n < 1$. When $n = 0$ and $n = 1$, $E_F = E_P$.

5 Bethe lattice. Transport properties

As mentioned in the introduction strong mutual influence of magnetic and transport properties is displayed most

clearly in the temperature dependence of the resistivity. The existing experimental data for the manganese oxides show the strong dependence of the resistivity on temperature immediately below the magnetic critical point T_K , and on the magnetic field [10] (for old papers on this subject see in [17]).

Recently, the authors of a series of papers [10–12,14] have pointed out that the temperature-dependent transport properties can be scaled to a universal curve as a function of the magnetization. This universal formula for the resistivity was obtained by Furukawa in the frame of the double exchange model with the classical localized spins ($S \rightarrow \infty$). For small values of magnetization m and the Lorentzian density of states of itinerant electrons this formula has the form [12]

$$\frac{\rho(0) - \rho(m)}{\rho(0)} = Cm^2, \quad (5.1)$$

where

$$C = \frac{8 - \cos(2\pi(1 - n))}{2 - \cos(2\pi(1 - n))} \quad (5.2)$$

is the coefficient depending on electron concentration, but it does not depend on temperature.

However, it should be noted that from a theoretical point of view magnetization can not serve as fundamental quantity. Indeed, in a wide temperature region the behaviour of the magnetization can depend on different parameters of theory. In particular, in our double exchange model the temperature behaviour of the magnetization at $n = 0.5$ essentially differs from that at $n = 0.99$ (see Fig. 7).

In this section we shall calculate the resistivity of the double exchange Bethe lattice as a function of temperature directly. Unfortunately, this calculation will be made by numerical methods.

In infinite dimensions we have the following formula for conductivity [12,21–23]

$$\sigma_{dc} = \sigma_0 W^2 \int_{-\infty}^{\infty} d\varepsilon \rho_0(\varepsilon) \times \sum_{\sigma} \int_{-\infty}^{\infty} d\omega \left(-\frac{\partial f(\omega)}{\partial \omega} \right) A_{\sigma}^2(\varepsilon, \omega - \mu), \quad (5.3)$$

where the constant σ_0 gives the unit of conductivity, and

$$A_{\sigma}(\varepsilon, \omega) = -\frac{1}{\pi} \text{Im} \mathcal{G}_{\sigma}(\varepsilon, \omega + i\delta). \quad (5.4)$$

The chemical potential μ in (5.3) is defined from the formula (4.8) of Section 4.

In order to obtain the expression for the spectral function $A_{\sigma}(\varepsilon, \omega)$ let us present the one-particle Green's function in the Dyson form

$$\mathcal{G}_{\sigma}(\varepsilon, \omega) = \frac{1}{\omega + \mu - \varepsilon - \Sigma_{\sigma}(\omega)}, \quad (5.5)$$

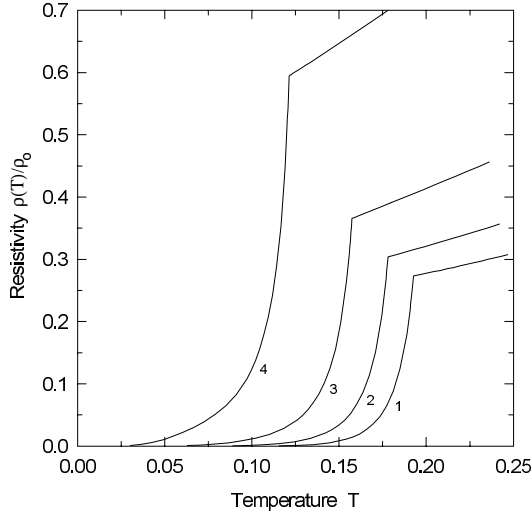


Fig. 10. Temperature dependence of resistivity, 1 – $n = 0.5$, 2 – $n = 0.7$, 3 – $n = 0.8$, 4 – $n = 0.9$.

where

$$\Sigma_{\sigma}(\omega) = (\omega + \mu) \frac{R_{\sigma}(\omega) - 1}{R_{\sigma}(\omega)}. \quad (5.6)$$

Taking into account the formula (4.3), we have

$$\Sigma_{\sigma}(\omega) = -\frac{1}{2} \left(\frac{1 - \sigma m}{1 + \sigma m} \right) \times \left\{ \omega + \mu + \sqrt{(\omega + \mu)^2 - \frac{1}{8} W^2 (1 + \sigma m)} \right\} \quad (5.7)$$

and

$$\text{Im } \Sigma_{\sigma}(\omega + i\delta) = -\frac{1}{2} \left(\frac{1 - \sigma m}{1 + \sigma m} \right) \times \sqrt{\frac{1}{8} W^2 (1 + \sigma m) - (\omega + \mu)^2} \quad (5.8)$$

for

$$-\frac{1}{2} W \sqrt{\frac{1}{2} (1 + \sigma m)} < \omega + \mu < \frac{1}{2} W \sqrt{\frac{1}{2} (1 + \sigma m)}. \quad (5.9)$$

Otherwise $\text{Im } \Sigma_{\sigma}(\omega + i\delta) = 0$.

Let us turn one's attention to the multiplier

$$\frac{1 - \sigma m}{1 + \sigma m}$$

in the expression (5.8). Firstly, the same multiplier is contained in the analogous expression for the self-energy part in [12]. Secondly, this multiplier provides exactly the decrease of resistivity when the magnetization m is increased. Indeed, in the limit $m \rightarrow 1$ (or $T \rightarrow 0$) we have

$$A_{\uparrow}(\varepsilon, \omega) = \delta(\omega + \mu - \varepsilon), \quad A_{\downarrow}(\varepsilon, \omega) = 0 \quad (5.10)$$

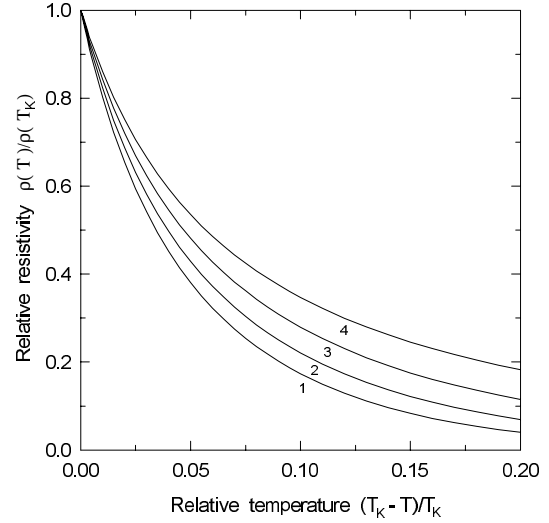


Fig. 11. Temperature dependence of relative resistivity immediately below the magnetic transition temperature T_K . 1 – $n = 0.5$, 2 – $n = 0.7$, 3 – $n = 0.8$, 4 – $n = 0.9$.

and the itinerant electron subsystem presents itself as a free electron gas.

The temperature-dependent resistivity $\rho(T)$ is shown in Figure 10, where $\rho_0 = 1/\sigma_0$ and T are expressed in units of $W/2$. For the numerical calculation of the resistivity from the formula (5.3), we have used the results of the calculations of the temperature-dependent magnetization (see Fig. 7).

One can see from Figure 10 that the resistivity reveals a sharp drop as temperature is decreased (or magnetization is increased) immediately below T_K . The breaking of the resistivity curve occurs at $T = T_K$ for each electron concentration n . In agreement with experimental data of $\text{La}_{1-x}\text{Sr}_x\text{MnO}_3$ (see Fig. 1 in [10]), the value of resistivity at $T = T_K$, $\rho(T_K)$, grows when the hole concentration $x = 1 - n$ is decreased.

The calculations for $n = 0.95$ and $n = 0.99$ show that the resistivity curve has a cusp at $T = T_K$ and immediately above T_K the resistivity decreased as temperature is increased. These curves are not shown in Figure 10.

In Figure 11 we show dependence of the relative resistivity $\rho(T)/\rho(T_K)$ on relative temperature $\tau = (T_K - T)/T_K$ immediately below T_K for different n . Using these resistivity curves we have constructed the formula, defining the behaviour of the relative resistivity as a function of τ . This formula has the form

$$\frac{\rho(T_K) - \rho(T)}{\rho(T_K)} = a\tau^{\nu} (1 + b\tau + c\tau^2), \quad (5.11)$$

where $\tau < 1$.

The coefficients a , b , c and the exponent ν for different n are given in Table 1.

Actually, the exponent ν defines the critical behaviour of resistivity below the magnetic transition temperature T_K . If we suggest that magnetization $m \sim \sqrt{\tau}$ at $\tau \ll 1$, then our dependence of $\rho(T)/\rho(T_K)$ on m will

Table 1.

n	ν	a	b	c
0.5	0.9170	14.7018	-8.3062	29.5002
0.7	0.9289	13.8696	-8.0842	28.5324
0.8	0.9309	12.4146	-7.7448	26.9634
0.9	0.9348	11.1775	-7.6366	26.6344

differ slightly from Furukawa's dependence (5.1). We want to remember in connection with this that we have taken into account the temperature dependence of resistivity from the formula (5.3) and that of the chemical potential μ from the formula (4.8) completely. As a result we have the mentioned difference between (5.1, 5.11).

6 Conclusion

In this paper the simplified double exchange model with Hamiltonian (2.7) was investigated and the exact solution in infinite-dimensional space was obtained for it. Equations (3.8, 3.20) were solved for Bethe lattice with $z \rightarrow \infty$ and with the help of (3.22, 3.23) the magnetic properties of a localized spins subsystem were studied. Ferromagnetic alignment was found to be more advantageous at any finite concentration of charge carriers in this model.

The use of the above-mentioned equations for the low-dimensional space gives us the true mean-field approximation. The internal Weiss molecular field, exerted on a localized spin, is determined by the properties of the itinerant electrons subsystem. We can determine its force and dependence on concentration n by the magnitude of T_K . For Bethe lattice with $z \rightarrow \infty$, T_K is given by the formula (4.14).

Although the double exchange model presented here is essentially simpler than the model in [3], the author hopes that it considers the main special features of this phenomenon. It is important that this model gives us a opportunity to go significantly farther in the theoretical

investigation of the systems with the double exchange what can be found to be sufficient for the general comprehension of the theory of the systems of many interacting particles.

This work is supported by Russian Fond of Fundamental Research, project 96-02-16000.

References

1. P.W. Anderson, H. Hasegawa, Phys. Rev. **100**, 675 (1955).
2. P.-G. de Gennes, Phys. Rev. **118**, 141 (1960).
3. K. Kubo, N. Ohata, J. Phys. Soc. Jpn **33**, 21 (1972).
4. K. Kubo, J. Phys. Soc. Jpn **33**, 929 (1972).
5. N. Ohata, J. Phys. Soc. Jpn **34**, 343 (1973).
6. B.M. Letfulov, Fiz. Tv. Tela (USSR) **19**, 991 (1977).
7. G.H. Jonker, J.H. Van Santen, Physica **16**, 599 (1950).
8. C. Zener, Phys. Rev. **82**, 403 (1951).
9. S.V. Vonsovski, JETP, **16**, 981 (1946).
10. Y. Tokura, A. Urushibara, Y. Morimoto, T. Arima, A. Asamitsu, G. Kido, N. Furukawa, J. Phys. Soc. Jpn **63**, 3931 (1994).
11. N. Furukawa, J. Phys. Soc. Jpn **63**, 3214 (1994).
12. N. Furukawa, J. Phys. Soc. Jpn **64**, 2734 (1994).
13. N. Furukawa, J. Phys. Soc. Jpn **64**, 2754 (1994).
14. N. Furukawa, J. Phys. Soc. Jpn **64**, 3164 (1994).
15. W. Metzner, D. Vollhardt, Phys. Rev. Lett. **62**, 324 (1989).
16. E. Muller-Hartmann, Z. Phys. B **74**, 507 (1989).
17. S. Methfessel, D.C. Mattis, *Handbuch der Physik*, XVIII/I, (Springer-Verlag, Berlin, Heidelberg, New-York, 1968) p.389
18. Yu.A. Izyumov, B.M. Letfulov, E.V. Shipitsyn, M. Bartkowiak, K.A. Chao, Phys. Rev. B **46**, 15697 (1992).
19. U. Brandt, C. Mielsh, Z. Phys. B **75**, 365 (1989).
20. E. Nagaev, *Fizika magnitnyh poluprovodnikov* (Nauka, Moskva, 1979).
21. A. Khurana, Phys. Rev. Lett. **64**, 1990 (1990).
22. G. Möller, A. Ruckenstein, S. Schmitt-Rink, Phys. Rev. B **46**, 7427 (1992).
23. Th. Pruschke, D.L. Cox, M. Jarrel, Phys. Rev. B **47**, 3553 (1993).